Int J Clin Exp Med 2020;13(6):4042-4051
www.ijcem.com /ISSN:1940-5901/IJCEM0107859

Original Article

miR-132-3p regulates notch signaling to relieve neuropathic pain in rats

Yi Cen[1*], Tengfei Zhu[2*], Yue Wang[1], Zhe Zhang[1], Hui Chen[1]

[1]Department of Pain Management, Shanghai Fourth People's Hospital Affiliated to Tongji University School of Medicine, Shanghai, China; [2]Department of Anesthesiology, Changzheng Hospital, Second Military Medical University, Shanghai, China. [*]Equal contributors.

Received January 14, 2020; Accepted March 3, 2020; Epub June 15, 2020; Published June 30, 2020

Abstract: Objective: To explore the effects of miR-132-3p and Notch signaling on neuropathic pain in rats. Methods: A neuropathic pain model was established in rats and mechanical and thermal pain thresholds were assessed. The expression of glial fibrillary acidic protein (GFAP) and microglial marker OX-42 (CD11b) were investigated by immunofluorescence. Spinal cord cell apoptosis was assessed by TUNEL staining. Dual luciferase reporter assays were used to confirm the relationship between miR-132-3p and Notch 1. QRT-PCR and western blot were used to detect miRNA and protein expression, respectively. Results: We found that miR-132-3p targeted and negatively regulated Notch 1 expression. The overexpression of miR-132-3p and/or the inhibition of Notch signaling increased the thermal and mechanical pain thresholds (both $P<0.05$), GFAP and OX-42 expression (both $P<0.05$) and decreased the rates of apoptosis in spinal cord cells ($P<0.05$). The activation of Notch alleviated the protective effects of miR-132-3p. Conclusion: The overexpression of miR-132-3p inhibits Notch signaling and relieves neuropathic pain in rats.

Keywords: miR-132-3p, notch signaling, neuropathic pain

Introduction

Neuropathic pain is both chronic and prevalent pathological pain caused by injury to the central nervous system [1-3]. Over 8% of the population suffers from neuropathic pain and it continues to increase in prevalence due to an aging population [4, 5]. Disease onset seriously affects the quality of life of patients. Clinically, conventional analgesics can alleviate pain in the short term, but fails to effectively prevent and cure pain [6, 7]. The pathogenesis of neuropathic pain remains complex and largely undefined [8, 9]. Exploring the regulatory mechanism(s) of neuropathic pain can provide a theoretical basis for its effective treatment.

Notch is a key regulator of cellular function in vertebrates [10]. Notch signaling regulates the development of an array of tissues and organs, including blood vessels, muscles, peripheral nerves and central nerves. Under physiological conditions, Notch signaling plays a key role in neuronal excitation or inhibition [11-13]. The activation of Notch signaling leads to the excitation of neurons and increases their sensitivity to pain [14]. When exploring the upstream regulatory factors of Notch signaling, Targetscan revealed a binding site between miR-132-3p and Notch 1. MiR-132-3p is located on human chromosome 17 and is dysregulated in liver cancer, colorectal cancer, and gastric cancer [15-18]. MiR-132 is known to be downregulated in neuropathic pain, but its regulatory mechanism (s) remain poorly defined [19].

In this study, we established a neuropathic pain model in rats to explore the changes in miR-132-3p expression in neuropathic pain and its regulatory mechanisms.

Materials and methods

Ethics statement

This study was approved by the Ethics Committee of Shanghai Fourth People's Hospital Affiliated with Tongji University School of Medicine. All zoological experiments followed the international standards for laboratory animals.

Research objectives

Specific pathogen Free (SPF) grade male rats were purchased from the Guangdong Medical Animal Experimental Center (n=120). The average weight of the selected SD rats was 197.46± 13.76 g. Rats were fed in the animal room, exposed to 12 h light, and housed at 25°C. All rats had a normal diet and free access to water.

Establishment and grouping of neuropathic pain model in rats

The rats were divided into six groups: (1) normal (normal rats); (2) sham (sham operated rats); (3) model (model rats); (4) miR-132-3p mimic (model rats, overexpressing miR-132-3p via lentiviral vectors); (5) DAPT (model rats, notch inhibitor treated); and (6) miR-132-3p mimic + DAPT (model rats, combined processed). Drugs were purchased from the MCE company. Neuropathic pain models were established after one week of adaptive feeding. Twenty rats were left as controls. Rats were anesthetized by intraperitoneal injection of 1% pentobarbital sodium at a dose of 40 mg/kg. Rats were fixed on the operating table and the skin in the middle of the left leg was cut open, the biceps femoris muscle was peeled, and the left sciatic nerve was exposed. Ligation was performed at 1 mm intervals at the proximal end of the exposed sciatic nerve. The wound was then sutured. Operational procedures were identical in sham groups compared to model rats, but no ligations were performed. The normal group remained untreated. Following operation, rats in each group were intrathecally injected at T9 and T13 under anesthesia, and every 2-days thereafter (80 ng dose). After 14 days of modeling, rats were assessed for pain sensitivity. Following experimentation, rats were sacrificed through the removal of the tails and spinal cord, and tissues were extracted for subsequent analysis.

Thermal pain and mechanical pain threshold detection

Thermal pain and mechanical pain thresholds of all rats were measured using the hot-plate method and foot tactile instruments on the day prior to modeling, and on the 14th day of modeling. Hot plate tests were performed as follows: rats were placed on a glass plate with high heat conduction and were surrounded by a plexiglass enclosure. Rats were adapted to the partitioned environment and the heat intensity of the instrument was set at 40% and aligned with the soles of the paws. The time from initial exposure to retraction was recorded [20].

Mechanical pain thresholds were recorded as follows: Rats were placed on the partitioned floor of a foot tactile tester formed of a stainless steel mesh. The maximum touch force of the instrument was set to 50 g and the time was set to 5 s. Once the rats had adapted to the partitioned environment, the instruments were initiated until the needle contacted the feet of the rats. The contact force (g) of the rats from the instrument needle to foot retraction was recorded as a measurement of mechanical pain threshold.

Immunofluorescence

Astrocytes from rat spinal cord tissue sections were labeled with GFAP and rat microglia were labeled with OX-42. Briefly, sections were probed with rabbit anti-GFAP (ab33922, Abcam, USA) and rat anti-OX-42 (ab1211, Abcam, USA) for 1 h at room temperature. Sections were then washed in PBS and labeled with goat anti-rabbit IgG-FITC (ab6717, Abcam, USA) or goat anti-rat IgG-FITC (ab6785, Abcam, USA) for 30 min. Cell nuclei were DAPI stained (Invitrogen molecular probes, Carlsbad, CA, USA) for 10 min, and slides were mounted using anti-fluorescence quenching agent. Slides were imaged under a fluorescence microscope (XSP-BM-22AY, Shanghai Optical Instrument Factory, Shanghai, China).

TUNEL staining

Six sections of spinal cord tissues were taken from each group of rats to detect the rates of apoptosis in the spinal cord tissue. Sections were placed onto slides and numbered. After dewaxing and hydration, sections were washed twice in PBS and labeled with TUNEL reagent in a wet-box at room temperature for 1 h. Sections were then DAPI stained and imaged on a fluorescent microscope (Nikon TE2000, Tokyo, Japan). TUNEL-positive cells were quantified using Image-pro Plus 6.0 software from five random fields of view.

Dual luciferase assays

The binding sites of miR-132-3p and Notch 1 were predicted using www.targetscan.org. For

Table 1. qRT-PCR primer sequence

Gene	Sequence (5'-3')
miR-132-3p	
Upstream	ATGGCTGTAGACTGTT
Downstream	ACGTCTATACGCCCA
U6	
Upstream	CGCTTCGGCAGCACATATAC
Downstream	TTCACGAATTTGCGTGTCAT
Notch 1	
Upstream	CTGTCCCGTGTCAAGCTGAT
Downstream	CCATCCTGGGTTGTGCTCTT
NICD	
Upstream	CGATATCGTGCGGCTTTTGG
Downstream	GGTGAGGCCACATCTGACAA
GAPDH	
Upstream	TGTGAACGGATTTGGCCGTA
Downstream	GATGGTGATGGGTTTCCCGT

dual luciferase reporter assays, Notch 1 was mutated at the miR-132-3p binding site and WT or mutant plasmids were transfected into HEK293T cells with Renilla luciferase controls and miR-132-3p mimic or NC plasmids. Cells were lysed after 24 h and Firefly and Renilla activity were measured (Promega). Relative luciferase activity was obtained from the ratio of firefly to Renilla luciferase.

QRT-PCR

Spinal cord tissues of each group of rats were homogenized and total RNA was isolated using the ultrapure RNA Extraction Kit (D203-01, GenStar Biosolutions Co., Ltd., Beijing, China). RNA was reverse transcribed with TaqMan MicroRNA Assays Reverse Transcription Primer (batch No. 4366596, Thermo Scientific, Waltham, MA, USA). Reaction conditions were set as 42°C, 30-50 min, 85°C and 5 s, miR-132-3p, U6, Notch 1, NICD and GAPDH primers were synthesized by Sangon Biotech (Shanghai) Co., Ltd. (**Table 1**). U6 was used as an internal reference for miR-132-3p and GAPDH was used as a reference for Notch 1 and NICD. Fluorescent qPCR was performed using SYBR® Premix Ex TaqTM II Kit (RR820A, Xingzhi Biotechnology Co., Ltd., Jiangsu, China). The reaction system was as follows: 50 μL: SYBR® Premix Ex TaqTM II (2×) 25 μL, upstream primer 2 μL, downstream primer 2 μL, ROX Reference Dye (50×) 1 μL, DNA template 4 μL, and ddH2O 16 μL. Fluorescent qPCRs were performed on an ABI PRISM® 7300 (Prism® 7300, Shanghai Kunke Instrument and Equipment Co., Ltd., Shanghai, China) system. Reaction conditions were as follows: pre-denaturation at 95°C for 10 min, denaturation at 95°C for 15 s, annealing at 60°C for 30 s and extension at 72°C for 1 min (40 cycles). The $2^{-\Delta\Delta Ct}$ method was used to calculate the relative expression of each target gene (n=3). ΔΔCt = (mean CT value of each target gene in the experimental group - mean CT value of each reference gene in the experimental group) - (mean CT value of each target gene in the control group - mean CT value of each reference gene in the control group).

Western blot analysis

Total protein from rat spinal cord tissue was extracted using RIPA buffer (R0010, Beijing Solarbio Technology Co., Ltd., Beijing, China). Transfected cells were washed with precooled PBS and lysates (60% RIPA + 39% SDS + 1% protease inhibitor) were centrifuged at 4°C and 13500 rpm for 30 min. Protein concentrations were determined via BCA assay (Shanghai Jining Industry Co., Ltd., Shanghai, China) and proteins were resolved by SDS page electrophoresis (Shanghai Ruji Biotechnology Co., Ltd., Shanghai, China), voltage 100 V, electrophoresis 90 min. Proteins were wet-transferred to nitrocellulose membranes and blocked in 5% BSA for 1 h at room temperature. Membranes were labeled with rabbit anti-Notch 1 (ab8925, Abcam, USA), NICD (ab52301, Abcam, USA) and GAPDH (ab9485, Abcam, USA) overnight at 4°C and washed 5 times in PBS for 5 min. Membranes were labeled with HRP-conjugated goat anti-rabbit IgG antibodies (ab-150077, Abcam, USA) at room temperature and reacted with ECL (ECL808-25, Biomiga, USA) for 1 min. Membranes were washed and proteins bands were imaged using the ECL system (36209ES01, Qcbio Science & Technologies Co., Ltd., Shanghai, China). GAPDH was probed as a loading control.

Statistical analysis

SPSS 21.0 software (SPSS, Inc, Chicago, IL, USA) was used for data analysis. Measurement data were expressed as the mean ± SD. Independent sample t-tests were used for group comparisons. Welch tests were used for data calibration. The Shapiro Wilk method was used to test the normality of multiple groups of data.

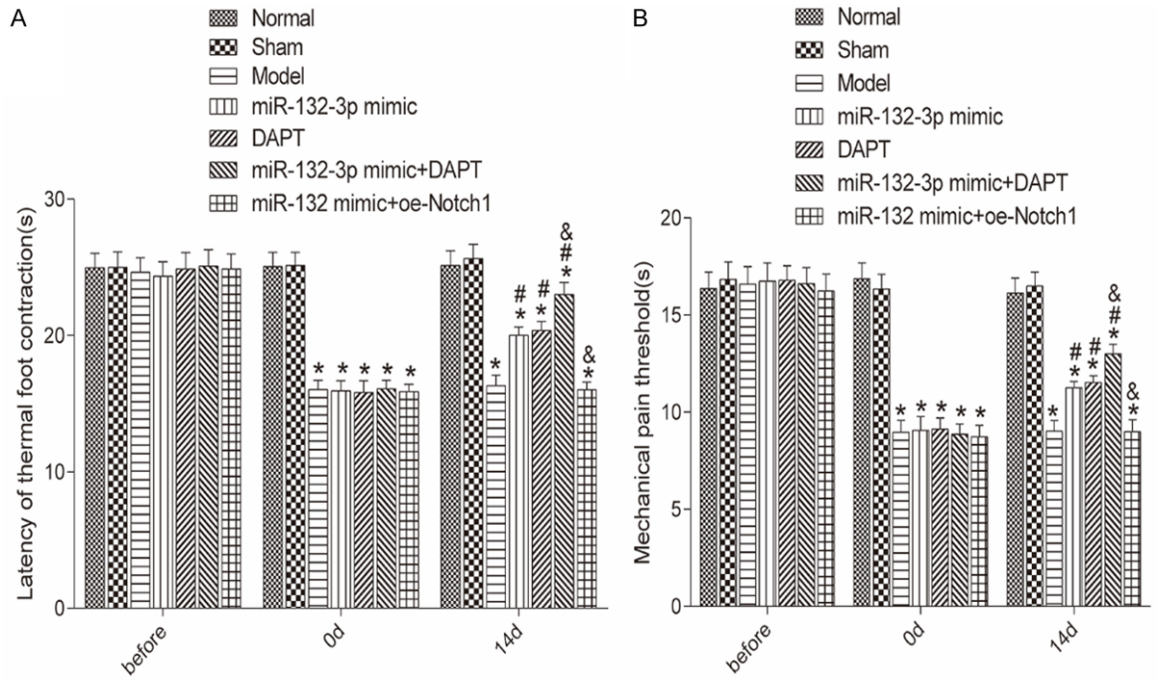

Figure 1. Thermal and mechanical pain threshold responses in rats. A: Thermal pain threshold responses in rats; B: Mechanical pain threshold responses in rats. Compared with normal group, *P<0.05; compared with model group, #P<0.05; compared with miR-132-3p mimic group; &P<0.05.

A univariate analysis of variance was used to analyze measurement data with a normal distribution. LSD was used to compare the mean values between multiple groups. Non-parametric Kruskal-Wallis tests were used to compare data that did not conform to a normal distribution. P<0.05 was deemed a significant difference.

Results

Thermal and mechanical pain threshold responses in rats

To explore the effects of miR-132-3p and Notch signaling on the pain tolerance of rats, we assessed the thermal pain threshold during thermal withdrawal latency (**Figure 1A**). Mechanical withdrawal thresholds were assessed following mechanical stimulation (**Figure 1B**). We found that, excluding the normal and sham group, the thermal withdrawal latency and mechanical pain threshold significantly decreased post-modeling (all P<0.05). On the 14th day of modeling, the thermal withdrawal latency and mechanical pain thresholds varied across the groups. Compared to the model group, the thermal withdrawal latency and mechanical pain threshold of rats in the miR-132-3p mimic and DAPT groups significantly increased (both P<0.05). Compared to the miR-132-3p mimic group, the thermal withdrawal latency and mechanical pain threshold of the miR-132-3p mimic + DAPT group were significantly higher, whilst the thermal withdrawal latency and mechanical pain threshold of the miR-132 mimic ± oe-Notch 1 group were significantly lower (all P<0.05). These data suggested that the overexpression of miR-132-3p and/or the inhibition of Notch signaling improved the thermal and mechanical pain thresholds of rats. The combined overexpression of miR-132-3p and Notch inhibition were most effective.

Astrocytes and microglia damage assessments

The activation of astrocytes and microglia leads to enhanced pain sensitivity. We assessed the levels of GFAP (**Figure 2A** and **2B**) and OX-42 (**Figure 2C** and **2D**) expression in each group through immunofluorescence labeling. Compared to the normal group, the expression of GFAP and OX-42 in the spinal cords of rats in all groups, except for the sham group, were significantly higher (all P<0.05). Compared to the model group, the expression of GFAP and OX-42

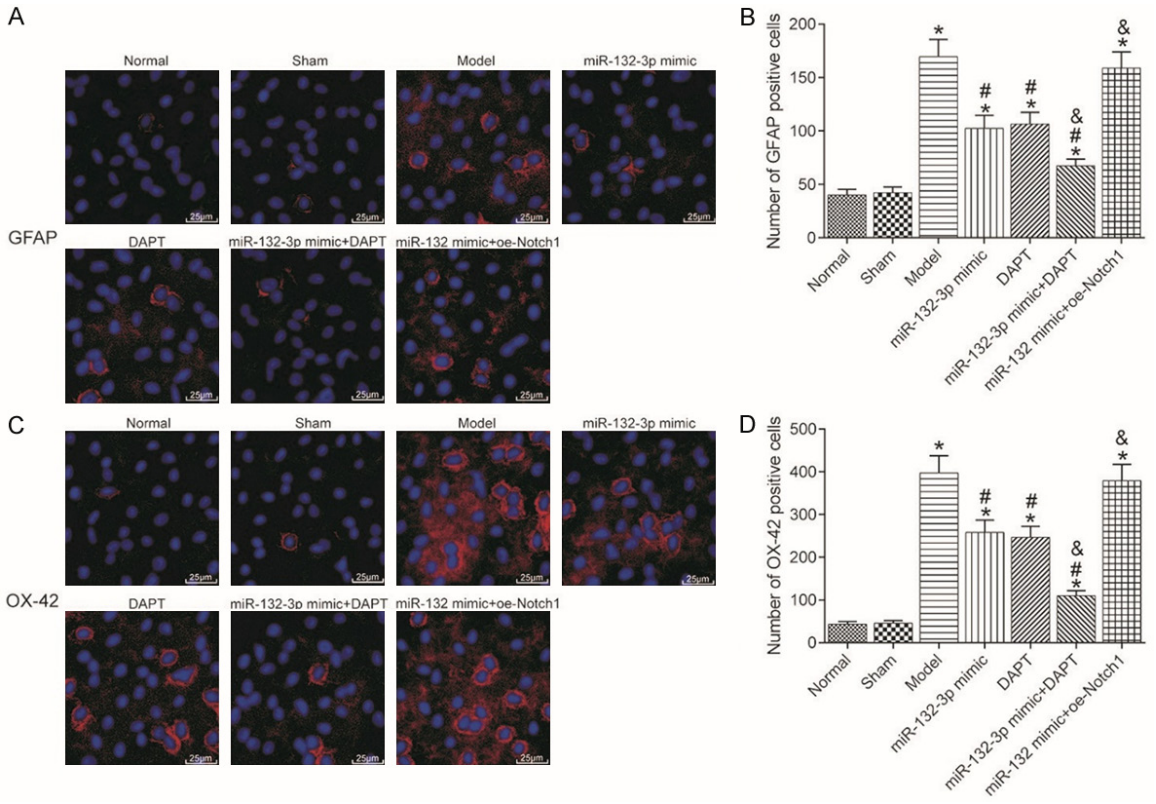

Figure 2. The expression levels of GFAP and OX-42 in the spinal cords of rats. A: The expression of GFAP detected by immunofluorescence; B: Statistical analysis of GFAP fluorescence expression; C: The expression of OX-42 detected by immunofluorescence; D: Statistical analysis of OX-42 fluorescence expression. GFAP, glial fibrillary acidic protein. Compared with normal group, *P<0.05; compared with model group, #P<0.05; compared with miR-132-3p mimic group; &P<0.05.

in miR-132-3p mimic and DAPT groups were significantly reduced (all P<0.05). Compared to the miR-132-3p mimic group, the expression of GFAP and OX-42 in miR-132-3p mimic + DAPT groups were significantly lower, whilst the expression of GFAP and OX-42 in the miR-132-3p mimic ± oe-Notch 1 group were significantly higher (all P<0.05). These results indicated that the overexpression of miR-132-3p or the inhibition of Notch signaling inhibited the activation of astrocytes and microglia.

Apoptosis of spinal cord cells

To detect apoptosis in the spinal cord cells, TUNEL staining was performed (**Figure 3**). Compared to the normal group, the apoptosis rates of spinal cord cells in all groups excluding the sham group significantly increased (all P<0.05). Compared to the model group, the apoptosis ratio of miR-132-3p mimic and DAPT groups decreased significantly (both P<0.05). Moreover, compared to the miR-132-3p mimic group, the apoptosis rates of miR-132-3p mimic + DAPT groups were significantly lower, whilst those of miR-132 mimic + oe-Notch 1 groups were significantly higher (P<0.05). These data suggested that the overexpression of miR-132-3p or the inhibition of Notch signaling prevented apoptotic induction in the spinal cord cells.

miR-132-3p regulates notch signaling

Dual luciferase reporter assays were performed to investigate the effects of miR-132-3p on Notch 1. Binding sites between miR-132-3p and Notch 1 were identified using Targetscan (**Figure 4A**). Dual luciferase reporter assays showed that, compared to NC mimics, the fluorescence intensity of miR-132-3p mimics significantly decreased following the co-transfection with Notch 1-WT, indicating an interaction (**Figure 4B**). The expression of miR-132-3p and Notch 1 in the spinal cord cells of each group were assessed by qRT PCR and western blot. The results showed that, compared to the nor-

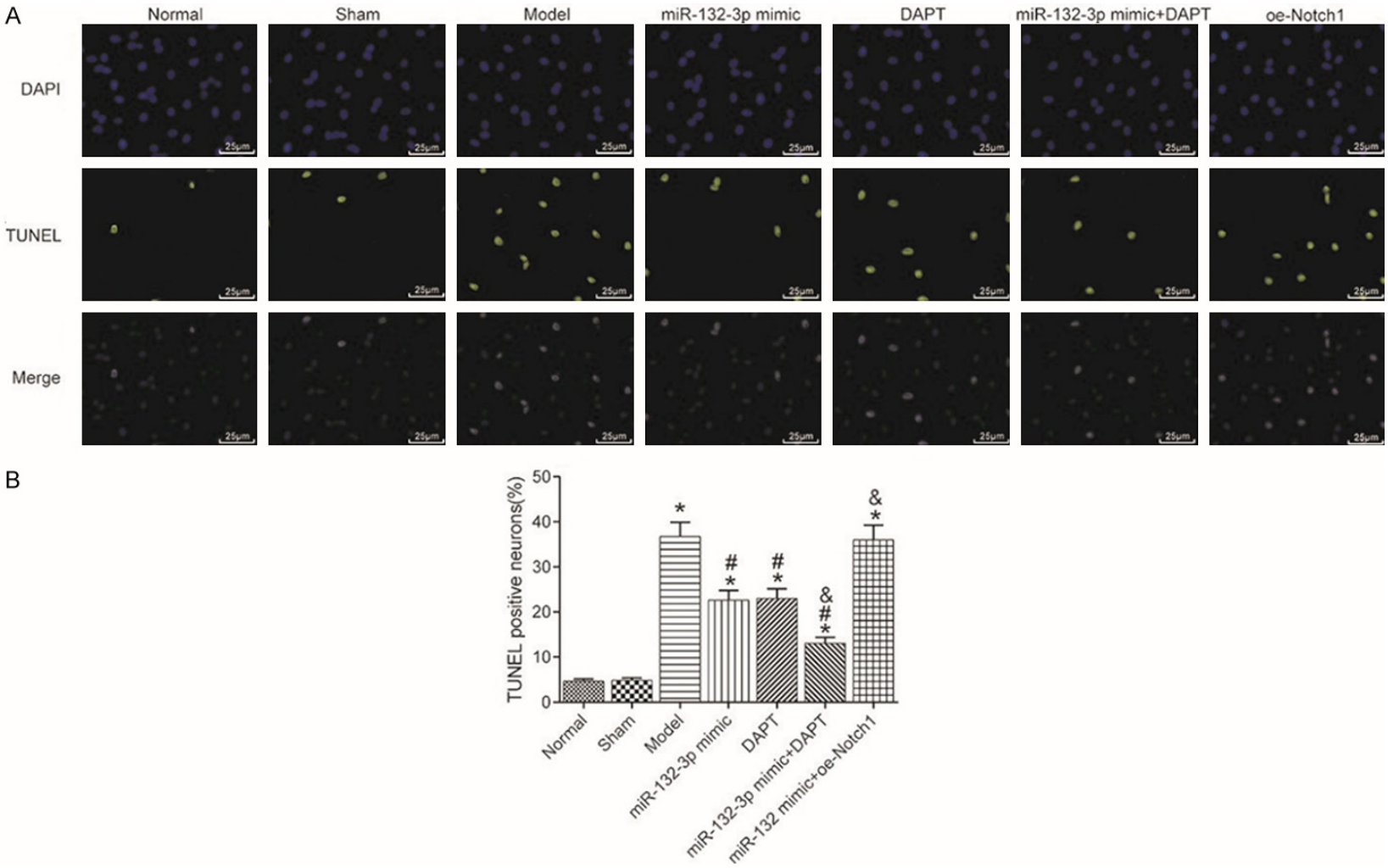

Figure 3. Comparison of apoptosis of spinal cord cells. A: TUNEL staining; B: The ratio of apoptosis of spinal cord cells. Compared with normal group, *P<0.05; compared with model group, #P<0.05; compared with miR-132-3p mimic group; &P<0.05.

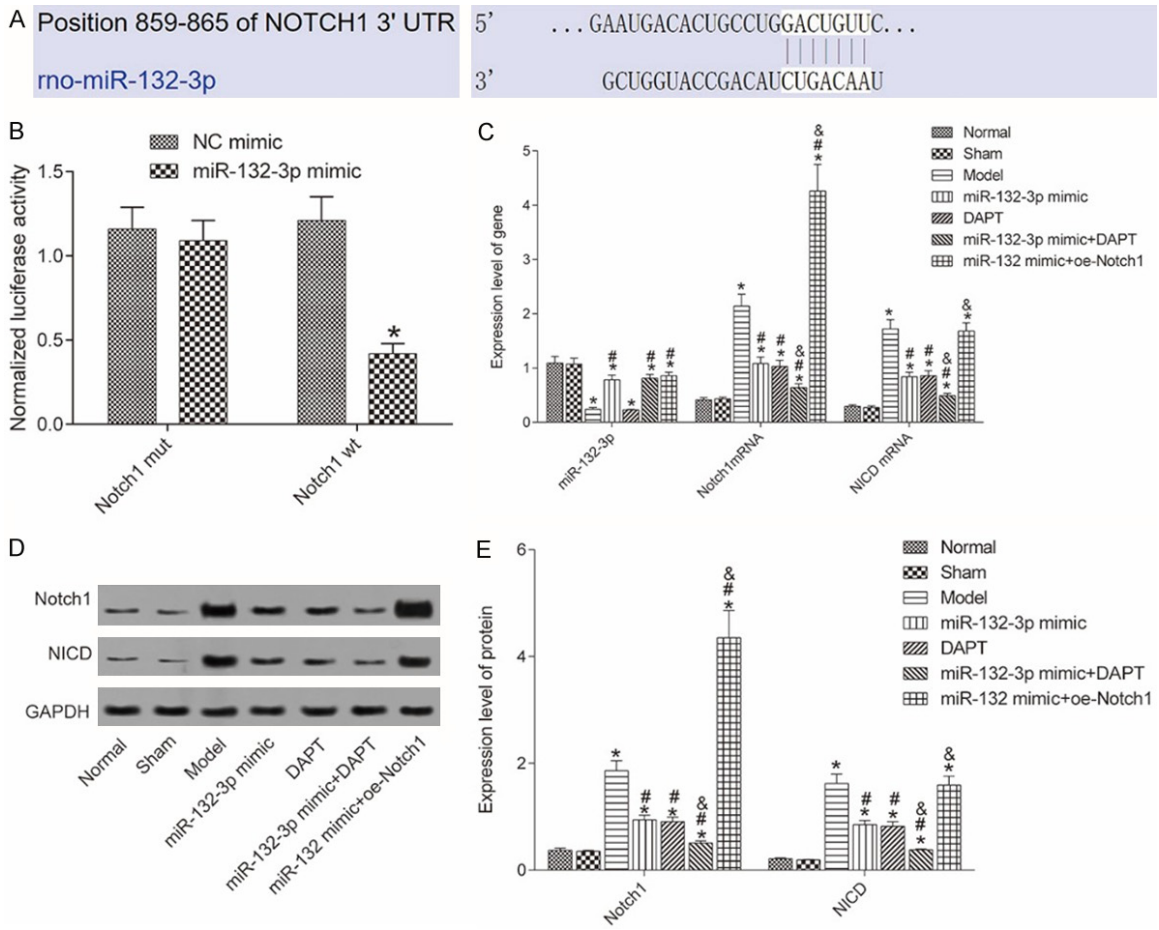

Figure 4. The regulatory mechanism of miR-132-3p and Notch signal pathway. A: The binding sites of miR-132-3p and Notch 1 predicted by Targetscan; B: The targeting relationship between miR-132-3p and Notch 1 confirmed by the dual luciferase assay; C: The expression of miR-132-3p, Notch 1 and NICD detected by qRT-PCR; D: Western blot results; E: The statistics of Notch 1 and NICD expression. Compared with normal group, *P<0.05; compared with model group, #P<0.05; compared with miR-132-3p mimic group; &P<0.05.

mal group, the expression of miR-132-3p in all groups excluding the sham group, significantly decreased, whilst the expression of Notch 1 and NICD significantly increased (all P<0.05). Compared to the model group, the expression of Notch 1 and NICD decreased in the miR-132-3p mimic group (P<0.05). There were no significant changes in miR-132-3p expression in the DAPT group, but the expression of Notch 1 and NICD decreased (P<0.05). Notch 1 and NICD levels were also lower in the miR-132-3p mimic + DAPT group (P<0.05), but increased in the miR-132 group (P<0.05). Compared to the miR-132-3p mimic group, miR-132-3p mimic + DAPT groups showed no changes in miR-132-3p levels (P>0.05), but the expression of Notch 1 and NICD significantly decreased (all P<0.05). MiR-132-3p expression in the miR-132 mimic + oe-Notch 1 group showed no significant changes (P>0.05), whilst the expression of Notch 1 and NICD increased (all P<0.05).

Discussion

Neuropathic pain is a common pathological disease. To-date, the pathogenesis of neuropathic pain remains poorly defined. In the clinic, the treatment of neuropathic pain involves drug analgesia which is not curative [21]. The occurrence of neuropathic pain impacts the quality of life of those afflicted. Exploring the pathogenesis of neuropathic pain provides a theoretical basis for clinical treatments with profound significance for radical treatment strategies.

To-date, studies have reported that Notch 1 signaling plays an important regulatory role in the

development of the nervous system [22]. Following ligand stimulation, the intracellular segments of Notch receptors (NICD) are separated [23] and bind to downstream transcription factors to promote the expression of downstream genes that regulate cell proliferation and apoptosis [24-26]. DAPT, an inhibitor of Notch signaling, prevents the neuropathic pain caused by nerve injury in rats in response to Notch activation [27, 28]. Xu et al. suggested that blocking Notch signaling can improve autoimmune neuritis [29]. Yang et al. showed that the inhibition of Notch signaling in the spinal cord of rats can inhibit diabetic neuropathy [30]. In this study, we assessed Notch 1 and NICD in normal and neuropathic pain models. The results showed that the expression of Notch 1 and NICD at the mRNA and protein level significantly increased in neuropathic pain models in rats. In addition, following DAPT treatment, pain sensitivity, astrocyte and microglia activation, and the apoptotic ratio of spinal cord cells were significantly reduced. These results were consistent with the finding that Notch signaling aggravates neuropathic pain and may be related to enhanced apoptosis and pain transmission of spinal neurons.

To explore the upstream regulatory factors of Notch signaling, we screened miR-132-3p binding partners using Targetscan. A binding site between miR-132-3p and Notch 1 was identified and confirmed through dual luciferase reporter assays. To-date, studies on miR-132-3p have focused on oncology, whilst the regulatory roles of miR-132-3p in the nervous system have rarely been studied. Leinders and Majer and colleagues suggested that miR-132-3p had a positive effect on neuropathic pain [31, 32]. In this study, we detected the expression of miR-132-3p in the spinal cord of normal and neuropathic pain modeled rats. We found that the expression of miR-132-3p was down-regulated in diseased rats whilst the pain sensitivity of diseased rats was significantly improved following the overexpression of miR-132-3p. In addition, after the treatment of miR-132-3p and DAPT, pain sensitivity improved and the apoptosis of spinal cord cells was significantly reduced. These results indicated that miR-132-3p alleviates neuropathic pain in rats through the inhibition of pain transmission and neuronal apoptosis, through inhibiting Notch signaling.

In summary, we have confirmed that miR-132-3p reduces neuropathic pain in rats through Notch inhibition, providing new insight into the pathogenesis of neuropathic pain in rats. Other target genes of miR-132-3p are likely to contribute to the regulation of neuropathic pain.

Disclosure of conflict of interest

None.

Address correspondence to: Hui Chen, Department of Pain Management, Shanghai Fourth People's Hospital Affiliated to Tongji University School of Medicine, No. 1878 Sichuan North Road, Shanghai 200003, China. Tel: +86-13003131393; Fax: +86-021-56663031; E-mail: chenhui8ksi@163.com

References

[1] Irwin DJ, Grossman M, Weintraub D, Hurtig HI, Duda JE, Xie SX, Lee EB, Van Deerlin VM, Lopez OL, Kofler JK, Nelson PT, Jicha GA, Woltjer R, Quinn JF, Kaye J, Leverenz JB, Tsuang D, Longfellow K, Yearout D, Kukull W, Keene CD, Montine TJ, Zabetian CP and Trojanowski JQ. Neuropathological and genetic correlates of survival and dementia onset in synucleinopathies: a retrospective analysis. Lancet Neurol 2017; 16: 55-65.

[2] Braak H and Del Tredici K. Neuropathological staging of brain pathology in sporadic Parkinson's disease: separating the wheat from the chaff. J Parkinsons Dis 2017; 7: S71-S85.

[3] Luo H, Huang Y, Du X, Zhang Y, Green AL, Aziz TZ and Wang S. Dynamic neural state identification in deep brain local field potentials of neuropathic pain. Front Neurosci 2018; 12: 237.

[4] Ferrero K, Silver M, Cocchetto A, Masliah E and Langford D. CNS findings in chronic fatigue syndrome and a neuropathological case report. J Investig Med 2017; 65: 974-983.

[5] Wang L, Xiaokaiti Y, Wang G, Xu X, Chen L, Huang X, Liu L, Pan J, Hu S, Chen Z and Xu Y. Inhibition of PDE2 reverses beta amyloid induced memory impairment through regulation of PKA/PKG-dependent neuro-inflammatory and apoptotic pathways. Sci Rep 2017; 7: 12044.

[6] Deseure K and Hans GH. Differential drug effects on spontaneous and evoked pain behavior in a model of trigeminal neuropathic pain. J Pain Res 2017; 10: 279-286.

[7] Pintore MD, D'Angelo A, Dondo A, Zoppi S, Mandola ML, Rizzo F, Costassa EV, Corona C, Casalone C and Iulini B. Neuropathological findings in equids during west nile disease sur-

veillance activities in Piedmont, Italy. J Comp Pathol 2017; 156: 71-71.
[8] D'Adamo P, Welzl H, Papadimitriou S, Raffaele di Barletta M, Tiveron C, Tatangelo L, Pozzi L, Chapman PF, Knevett SG, Ramsay MF, Valtorta F, Leoni C, Menegon A, Wolfer DP, Lipp HP and Toniolo D. Deletion of the mental retardation gene Gdi1 impairs associative memory and alters social behavior in mice. Hum Mol Genet 2002; 11: 2567-2580.
[9] Lee HJ, Jung KW, Chung SJ, Hong SM, Kim J, Lee JH, Hwang SW, Ryu HS, Kim MJ, Lee HS, Seo M, Park SH, Yang DH, Ye BD, Byeon JS, Choe J, Jung HY, Yang SK and Myung SJ. Relation of enteric alpha-synuclein to gastrointestinal dysfunction in patients with parkinson's disease and in neurologically intact subjects. J Neurogastroenterol Motil 2018; 24: 469-478.
[10] Wunderlich R, Lau P, Stein A, Engell A, Wollbrink A, Rudack C and Pantev C. Impact of spectral notch width on neurophysiological plasticity and clinical effectiveness of the tailor-made notched music training. PLoS One 2015; 10: e0138595.
[11] Kumar A, Huh TL, Choe J and Rhee M. Rnf152 is essential for NeuroD expression and delta-notch signaling in the zebrafish embryos. Mol Cells 2017; 40: 945-953.
[12] Baek C, Freem L, Goiame R, Sang H, Morin X and Tozer S. Mib1 prevents Notch Cis-inhibition to defer differentiation and preserve neuroepithelial integrity during neural delamination. PLoS Biol 2018; 16: e2004162.
[13] Yoon JH, Ann EJ, Kim MY, Ahn JS, Jo EH, Lee HJ, Lee HW, Lee YC, Kim JS and Park HS. Parkin mediates neuroprotection through activation of Notch 1 signaling. Neuroreport 2017.
[14] Das S and Knust E. A dual role of the extracellular domain of Drosophila Crumbs for morphogenesis of the embryonic neuroectoderm. Biol Open 2018; 7.
[15] Li G, Liu K and Du X. Long non-coding RNA TUG1 promotes proliferation and inhibits apoptosis of osteosarcoma cells by sponging miR-132-3p and upregulating SOX4 expression. Yonsei Med J 2018; 59: 226-235.
[16] Cai Y, Wang W, Guo H, Li H, Xiao Y and Zhang Y. miR-9-5p, miR-124-3p, and miR-132-3p regulate BCL2L11 in tuberous sclerosis complex angiomyolipoma. Lab Invest 2018; 98: 856-870.
[17] Weber DG, Gawrych K, Casjens S, Brik A, Lehnert M, Taeger D, Pesch B, Kollmeier J, Bauer TT, Johnen G and Bruning T. Circulating miR-132-3p as a candidate diagnostic biomarker for malignant mesothelioma. Dis Markers 2017; 2017: 9280170.
[18] He L, Qu L, Wei L, Chen Y and Suo J. Reduction of miR1323p contributes to gastric cancer proliferation by targeting MUC13. Mol Med Rep 2017; 15: 3055-3061.
[19] El Fatimy R, Li S, Chen Z, Mushannen T, Gongala S, Wei Z, Balu DT, Rabinovsky R, Cantlon A, Elkhal A, Selkoe DJ, Sonntag KC, Walsh DM and Krichevsky AM. MicroRNA-132 provides neuroprotection for tauopathies via multiple signaling pathways. Acta Neuropathol 2018; 136: 537-555.
[20] Gaudet AD, Ayala MT, Schleicher WE, Smith EJ, Bateman EM, Maier SF and Watkins LR. Exploring acute-to-chronic neuropathic pain in rats after contusion spinal cord injury. Exp Neurol 2017; 295: 46-54.
[21] Brouland JP, Sala N, Tusgul S, Rebecchini C and Kovari E. Bacillus cereus bacteremia with central nervous system involvement: a neuropathological study. Clin Neuropathol 2018; 37: 22-27.
[22] Li Q, Zhang X, Cheng N, Yang C and Zhang T. Notch 1 knockdown disturbed neural oscillations in the hippocampus of C57BL mice. Prog Neuropsychopharmacol Biol Psychiatry 2018; 84: 63-70.
[23] Hoseth EZ, Krull F, Dieset I, Morch RH, Hope S, Gardsjord ES, Steen NE, Melle I, Brattbakk HR, Steen VM, Aukrust P, Djurovic S, Andreassen OA and Ueland T. Attenuated Notch signaling in schizophrenia and bipolar disorder. Sci Rep 2018; 8: 5349.
[24] Zeng WX, Han YL, Zhu GF, Huang LQ, Deng YY, Wang QS, Jiang WQ, Wen MY, Han QP, Xie D and Zeng HK. Hypertonic saline attenuates expression of Notch signaling and proinflammatory mediators in activated microglia in experimentally induced cerebral ischemia and hypoxic BV-2 microglia. BMC Neurosci 2017; 18: 32.
[25] Mishra AK, Bernardo-Garcia FJ, Fritsch C, Humberg TH, Egger B and Sprecher SG. Patterning mechanisms diversify neuroepithelial domains in the drosophila optic placode. PLoS Genet 2018; 14: e1007353.
[26] Martin-Lanneree S, Halliez S, Hirsch TZ, Hernandez-Rapp J, Passet B, Tomkiewicz C, Villa-Diaz A, Torres JM, Launay JM, Beringue V, Vilotte JL and Mouillet-Richard S. The cellular prion protein controls notch signaling in neural stem/progenitor cells. Stem Cells 2017; 35: 754-765.
[27] Xie K, Qiao F, Sun Y, Wang G and Hou L. Notch signaling activation is critical to the development of neuropathic pain. BMC Anesthesiol 2015; 15: 41.
[28] Xie K, Jia Y, Hu Y, Sun Y, Hou L and Wang G. Activation of notch signaling mediates the induction and maintenance of mechanical allodynia in a rat model of neuropathic pain. Mol Med Rep 2015; 12: 639-644.

[29] Xu L, Li L, Zhang CY, Schluesener H and Zhang ZY. Natural diterpenoid oridonin ameliorates experimental autoimmune neuritis by promoting anti-inflammatory macrophages through blocking notch pathway. Front Neurosci 2019; 13: 272.

[30] Yang C, Gao J, Wu B, Yan N, Li H, Ren Y, Kan Y, Liang J, Jiao Y and Yu Y. Minocycline attenuates the development of diabetic neuropathy by inhibiting spinal cord notch signaling in rat. Biomed Pharmacother 2017; 94: 380-385.

[31] Leinders M, Uceyler N, Pritchard RA, Sommer C and Sorkin LS. Increased miR-132-3p expression is associated with chronic neuropathic pain. Exp Neurol 2016; 283: 276-286.

[32] Majer A, Medina SJ, Niu Y, Abrenica B, Manguiat KJ, Frost KL, Philipson CS, Sorensen DL and Booth SA. Early mechanisms of pathobiology are revealed by transcriptional temporal dynamics in hippocampal CA1 neurons of prion infected mice. PLoS Pathog 2012; 8: e1003002.